Focal Thickness Reduction of the Ganglion Cell-Inner Plexiform Layer Best Discriminates Prior Optic Neuritis in Patients With Multiple Sclerosis

Huiling Hu,[1,2] Hong Jiang,[2,3] Giovana Rosa Gameiro,[2] Jeffrey Hernandez,[3] Silvia Delgado,[3] and Jianhua Wang[2]

[1]Shenzhen Key Laboratory of Ophthalmology, Shenzhen Eye Hospital, Jinan University, Shenzhen, China
[2]Department of Ophthalmology, Bascom Palmer Eye Institute, University of Miami Miller School of Medicine, Miami, Florida, United States
[3]Department of Neurology, University of Miami Miller School of Medicine, Miami, Florida, United States

Correspondence: Hong Jiang, Bascom Palmer Eye Institute, University of Miami, Miller School of Medicine, 1638 NW 10th Avenue, McKnight Building - Room 202A, Miami, FL 33136, USA;
h.jiang@med.miami.edu.

Purpose. The goal was to visualize topographic thickness maps of the intraretinal layers and evaluate their discrimination abilities and relationships with clinical manifestations in patients with multiple sclerosis (MS) and a history of optic neuritis (ON).

Methods. Thirty patients with relapsing-remitting MS (34 eyes with a history of ON [MSON] and 26 non-ON fellow eyes [MSFE]) were recruited together with 63 age- and sex-matched controls (HC). Ultrahigh resolution optical coherence tomography was used to image the macula and the volumetric data set was segmented to yield six intraretinal layers. Topographic thickness maps were aligned and averaged for the visualization. The thickness maps were partitioned using the Early Treatment Diabetic Retinopathy Study (ETDRS) and related to Sloan low-contrast letter acuity (LCLA), Expanded Disability Status Scale (EDSS), and disease duration.

Results. Focal thickness reduction occurred in the macular retinal nerve fiber layer (mRNFL) and ganglion cell-inner plexiform layer (GCIPL), with the most profound reduction occurring in MSON eyes ($P < 0.05$). A horseshoe-like thickness reduction pattern (U Zone) in the GCIPL appeared in MSON. The thickness of the U Zone had better discrimination power than the ETDRS partitions (area under the curve = 0.97) and differentiated 96% of MSON from HC. The thickness of the U Zone was positively correlated to 2.5% LCLA ($r = 0.38$, $P < 0.05$) and 1.25% LCLA ($r = 0.57$, $P < 0.05$).

Conclusions. The horseshoe-like thickness reduction of the GCIPL appeared to be an ON-specific focal thickness alteration with the highest discrimination power of prior ON.

Keywords: ganglion cell-inner plexiform layer, multiple sclerosis, history of optic neuritis, topographic thickness map, focal thinning

Multiple sclerosis (MS), affecting more than 2.3 million people worldwide, is a chronic autoimmune neurological disorder of the central nervous system.[1] Early diagnosis and treatment may stop or reverse the disease progression.[2] Current imaging diagnostic criteria include lesions of the brain and spine, but not the optic nerve.[3] Clinical and subclinical optic neuritis (ON) are highly prevalent during the MS disease course,[3–5] and image markers for ON are in development. The eye is a window to the brain. Thinning of the peripapillary retinal nerve fiber layer (pRNFL) and ganglion cell-inner plexiform layer (GCIPL) as measured in vivo using spectral-domain optical coherence tomography (SD-OCT) represent optic nerve damage and correlate with neurodegeneration, therapeutic efficacy, and disease progression.[6–10] Recent studies suggested that intereye pRNFL and GCIPL thickness differences[11–13] identified a history of unilateral ON, which may demonstrate optic nerve lesions in patients with MS and facilitate the diagnosis. However, intereye thickness differences only provide moderate discrimination power and identify approximately 70% of ON from healthy controls (HC).[11,13,14]

This low sensitivity may be due to the drawbacks in the intereye approach. To use the intereye thickness difference method, the criterion of unilateral ON must be predetermined. However, it is hard to exclude subclinical ON clinically, which occurs with high incidence in patients with MS.[3–5] The averaged thicknesses of the GCIPL and pRNFL that are used in intereye approaches[11,13,14] may not be sensitive enough to identify optic nerve damage. Because the distribution of the neural fiber and ganglion cells are not even,[15–17] and the alterations in these neural layers are not even.[15,16] The average thicknesses of these layers using arbitrary partitions, such as the elliptical partition, which is commonly used in the clinic, may not well define the focal thickness alterations[11,13,14] and could render the moderate discrimination power when using the intereye thickness difference approach.

The visualization and quantitative analysis of topographic thickness patterns of intraretinal layers may identify the most profound focal thickness alterations and help in the development of sensitive markers of prior ON in patients with MS. A previous study of MS patients without a history of ON
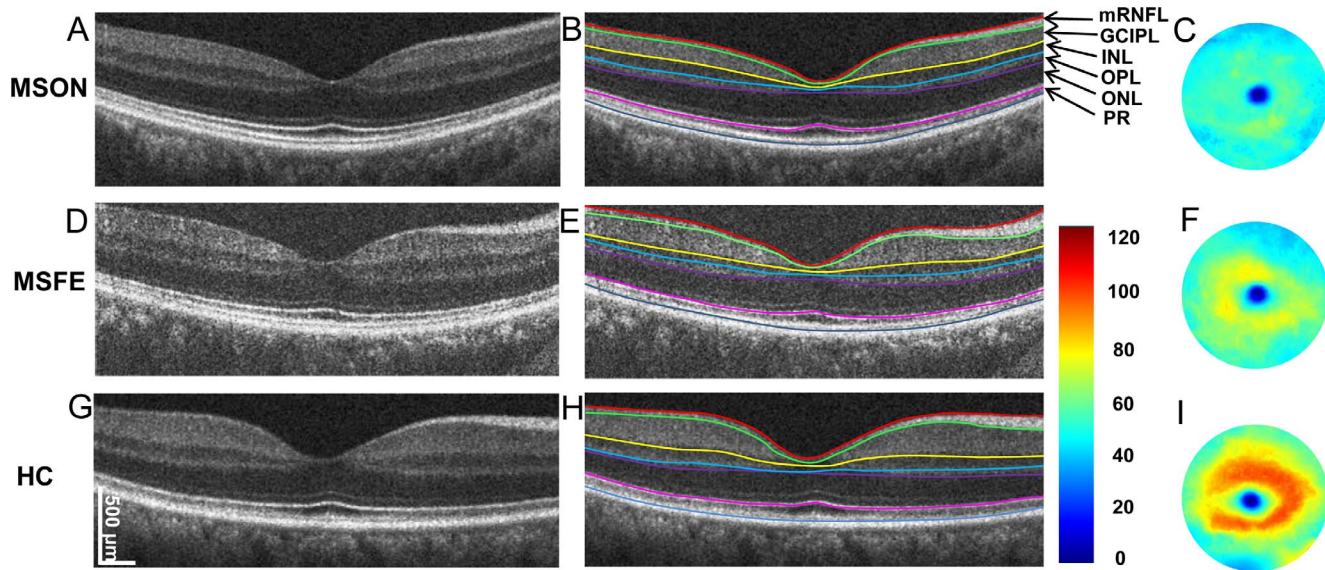
FIGURE 1. Cross-sectional retina and segmented topographic thickness maps of the GCIPL. Representative retinal images of MSON, MSFE, and HC groups were acquired using UHR-OCT with a 6-mm scan width (**A**, **D**, **G**). Six intraretinal layers with seven segmented boundaries were segmented (**B**, **E**, **H**). The corresponding GCIPL maps were created (**C**, **F**, **I**). *Bar unit*: μm.

(MSNON) reported that the most profound thickness alteration was located in the inferior nasal area of the GCIPL, named the "M Zone," and provided the highest discrimination power and strongest correlations to visual function and disease disability.[15] However, whether eyes with a history of ON in patients with MS share similar thickness patterns is not known. The purpose of the present study was to visualize the topographic thickness patterns of intraretinal layers and evaluate their discrimination performance and relationships with clinical manifestations in patients with MS and a history of ON.

METHODS

Participants

Thirty patients with relapsing-remitting MS and a history of ON were recruited (Table 1) from an ongoing observational cohort study of the Departments of Ophthalmology and Neurology at the University of Miami, Miller School of Medicine from July 2016 to March 2019. Patients were diagnosed according to the 2010 Revised McDonald Criteria.[18] There were a total of 34 eyes that had a history of ON (MSON) and 26 non-ON fellow eyes (MSFE). Four of the 30 patients had a history of bilateral ON. A total of 126 eyes from 63 age- and sex-matched healthy subjects were imaged as HC. The following exclusion criteria were used: any other systemic, ocular, or neurological diseases; refractive errors > ± 6.0 diopters; or relapse within the past 6 months.

The Institutional Review Board of the University of Miami approved this study, and all study subjects were treated

TABLE 1. Demographic Information

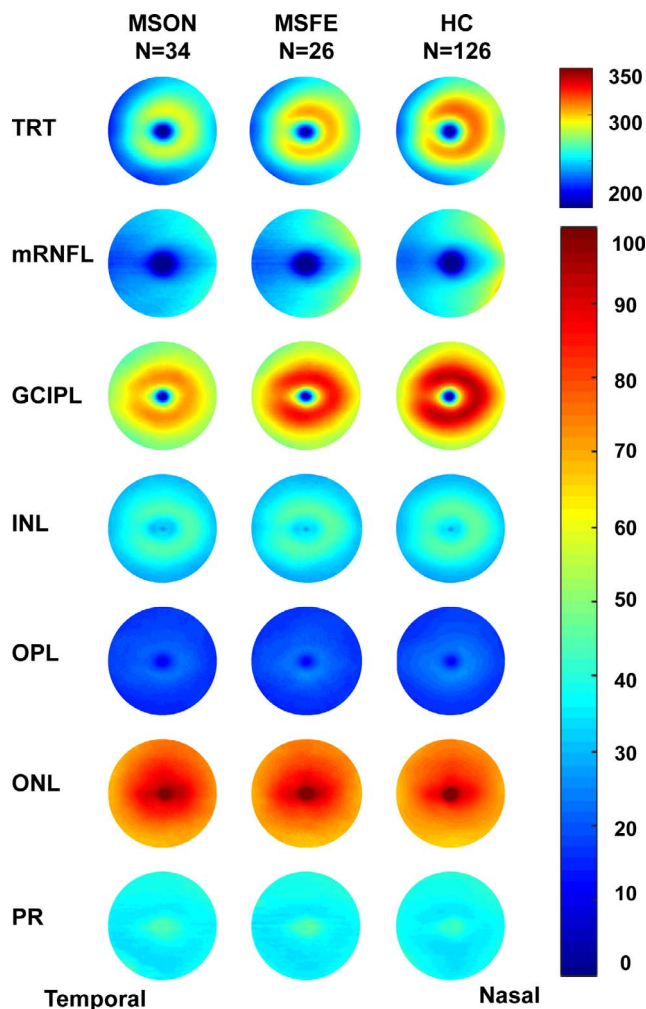|	**MS**	**HC**
Subjects	30	63
Age, y	39.6 ± 10.8	38.4 ± 10.7
Sex, male to female	7:23	22:41
EDSS	3.0 ± 2.2	
DD, y	9.1 ± 6.8	

DD, disease duration.

FIGURE 2. Intraretinal thickness maps. The topographic thickness of each retinal layer was averaged in each group. The topographic thickness maps of intraretinal layers showed an apparent trend of thickness reduction from HC to MSFE then MSON in the TRT, mRNFL, and GCIPL. *Bar unit*: μm.
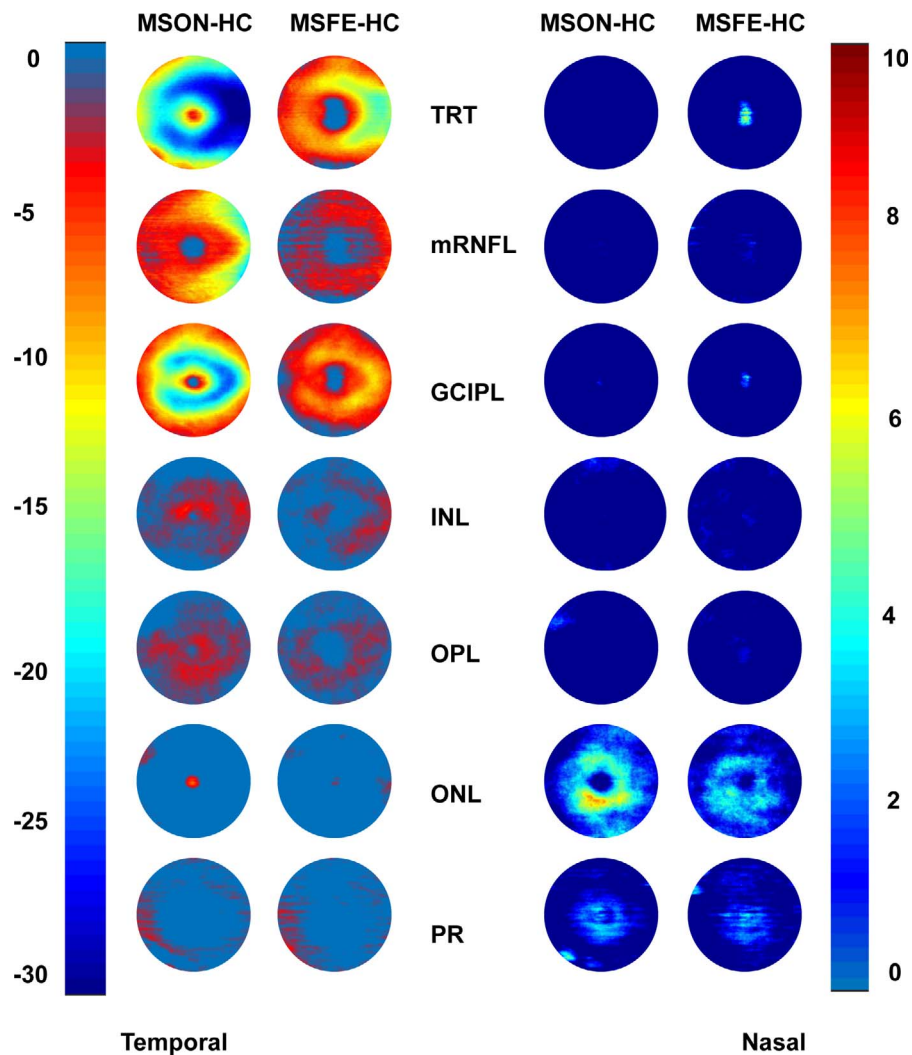
FIGURE 3. Alterations of intraretinal thickness maps. The differences between HC and MS eyes were visualized by subtracting the thickness of the HC group from the MS groups. The subtraction maps showed that the thickness reductions occurred in MSON and MSFE eyes in all intraretinal layers, except the ONL. *Bar unit*: μm.

according to the tenets of the Declaration of Helsinki. Each participant signed written informed consent after the details of the study were explained.

Each subject received a full eye examination, including best-corrected visual acuity (BCVA), color vision, intraocular pressure (IOP), and slit-lamp biomicroscopy of anterior and posterior segments. Binocular low-contrast letter acuity (LCLA) was tested using the 2.5% and 1.25% of the LCLA charts (low-contrast Sloan letter chart, Precision Vision, LaSalle, IL, USA) with the best possible correction for refractive errors. LCLA scores were quantified as the number of letters correctly read by the patient.[19] Most of the MS patients had a BCVA of 20/20 or above, normal color vision (tested using the Ishihara's color test), and confrontational visual field. However, the BCVA of one patient with bilateral ON was 20/40 bilaterally. Another patient had a BCVA of 20/50 for the MSON eye.

Topographic Thickness Maps of Intraretinal Layers Using Ultrahigh Resolution Optical Coherence Tomography (UHR-OCT)

As described previously,[16,17,20] the custom UHR-OCT system is a spectral domain OCT with an axial resolution of ∼3 μm in tissue

and a scan speed of 24,000 A-scans per second. The scan pattern was a raster scan with 512 A-scans (per B-scan) × 128 B-scans, which covered a field of view of 6 × 6 mm centered on the fovea. The scan data set was exported and segmented using an automatic image processing software program (Orion, Voxeleron LLC, Pleasanton, CA, USA).[17] Segmentation of all intraretinal layers of the horizontal scan (fast scan) and the vertical scan (slow scan) crossing the foveal center, and the thickness map of the total retina were exported and saved as a record for segmentation verification. However, the segmentation of each B-scan was not checked. The six segmented layers were the macular retinal nerve fiber layer (mRNFL), GCIPL, inner nuclear layer (INL), outer nuclear layer (ONL), outer plexiform layer (OPL), and retinal photoreceptor (PR). Total retinal thickness (TRT) was also recorded (Fig. 1).[20,21] The thickness measurements in annuli, quadrants, and sectors were exported using the Early Treatment Diabetic Retinopathy Study (ETDRS).

To visualize the topographical thickness pattern of each segmented intraretinal layer, thickness maps of each group were aligned using the center of the fovea and averaged. Maps of the left eyes were flipped horizontally and averaged with the maps of the right eyes. Differences between the thickness maps (i.e., 512 × 128 pixel array centered on the fovea) were calculated by
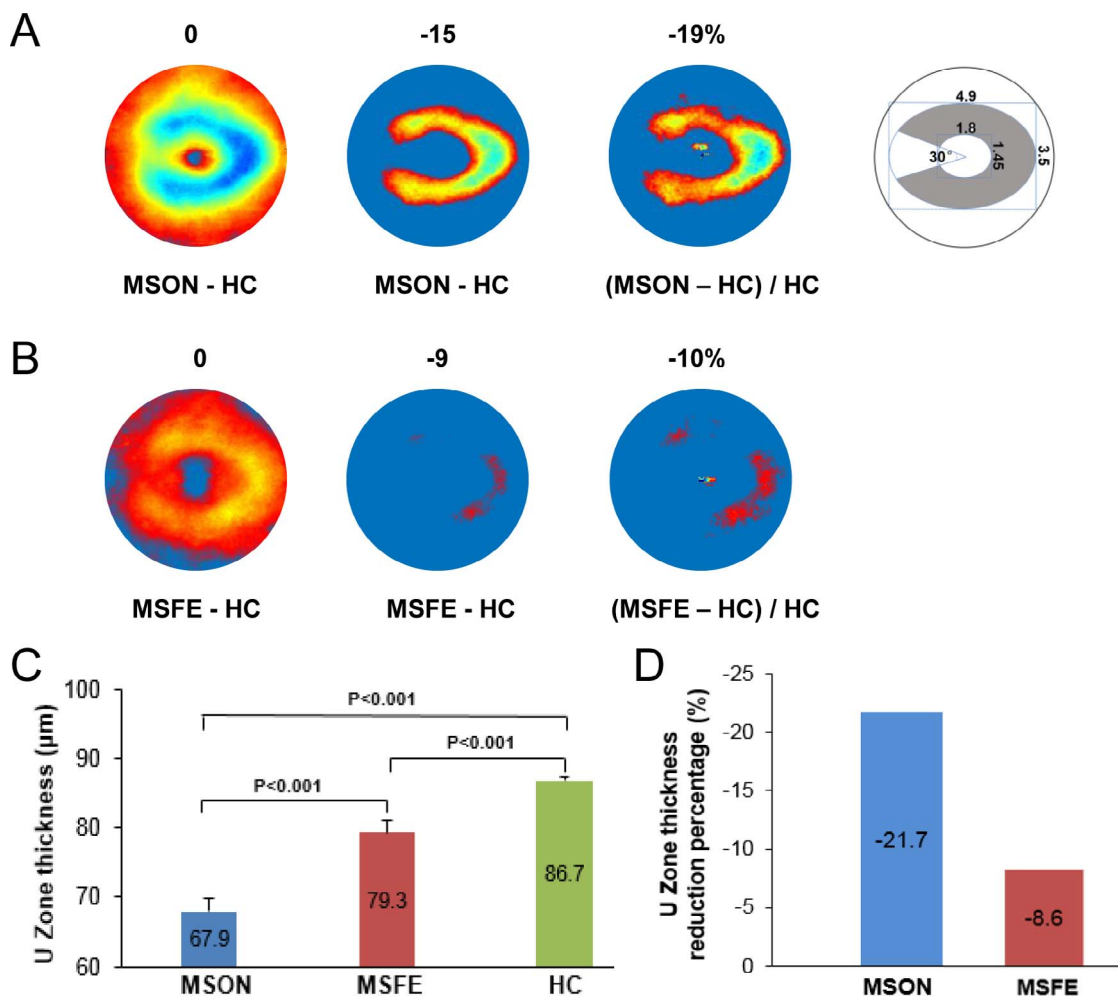
FIGURE 4. GCIPL thickness reduction patterns. Using different cutoff settings, the areas of focal thickness alterations were visualized in MSON (**A**) and MSFE (**B**) in comparison to HC. A horseshoe-like thickness reduction pattern was found in MSON (**A**). The schematic diagram shows the definition of the horseshoe shape of the thickness reduction, named as the "U Zone." The horseshoe-like thickness reduction was defined as the "U Zone" with a portion of an elliptic annulus (dimensions: 1.45 and 3.5 mm for the inner and outer vertical diameters, respectively, and 1.8 and 4.9 mm for the inner and outer horizontal diameters, respectively) around the fovea. In contrast, MSFE showed an island pattern located on the nasal side (**B**). GCIPL thickness (**C**) and proportional thicknesses (**D**) of the U Zone exhibited significant reductions in MSON compared with MSFE and HC. Similar horseshoe-like thickness reduction patterns were also evident in the proportional thickness maps, which were calculated as (MSON-HC)/HC and (MSFE-HC)/HC.

subtracting the thickness maps of control eyes from the thicknesses of the MSON or MSFE eyes to create thickness alteration maps.[16] Visualization was rendered using MATLAB software (version 2014b, MathWorks, Natick, MA, USA).

Statistical Analyses

Statistical Package for the Social Sciences (SPSS; version 25, IBM, Armonk, NY, USA) and Statistical Academic (version 13; TIBCO Software, Inc., Palo Alto, CA, USA) were used to analyze the data. Data are presented as the means ± standard error (SE). The sample size was calculated using a software program (Gpower, version 3.1.9). Based on the GCIPL thickness of the HC and MSON groups reported in previous studies,[11,13,14,22] a sample size of 20 subjects in each group would be sufficient to detect a true difference (10 μm) in GCIPL thickness with a detection power of 0.95. The present study, 63 HC and 30 MSON were recruited, and ensured sufficient power. The present study focused on the visualization of topographic thickness alterations in intraretinal layers, and this sample may be sufficient to determine the true alterations in a focal area

with the most profound alteration in thickness. Generalized estimating equation (GEE) models were used to quantify intercorrelation of eyes within subjects. Eyes (left or right) were set as within-subject variables. The thickness measurements including the GCIPL thickness of the U Zone were dependent variables. Age, sex, and eye were covariates in GEE models. In addition, disease duration and treatment (with and without treatment) were additional covariates in GEE models to analyze the differences between MSNON and MSON eyes. Relationships between thickness variables and clinical manifestations were analyzed using Pearson's correlation. $P < 0.05$ was considered statistically significant.

RESULTS

Topographic Thickness Maps of Intraretinal Layers

The topographic thickness maps of intraretinal layers showed an apparent trend of thickness reduction from HC to MSFE
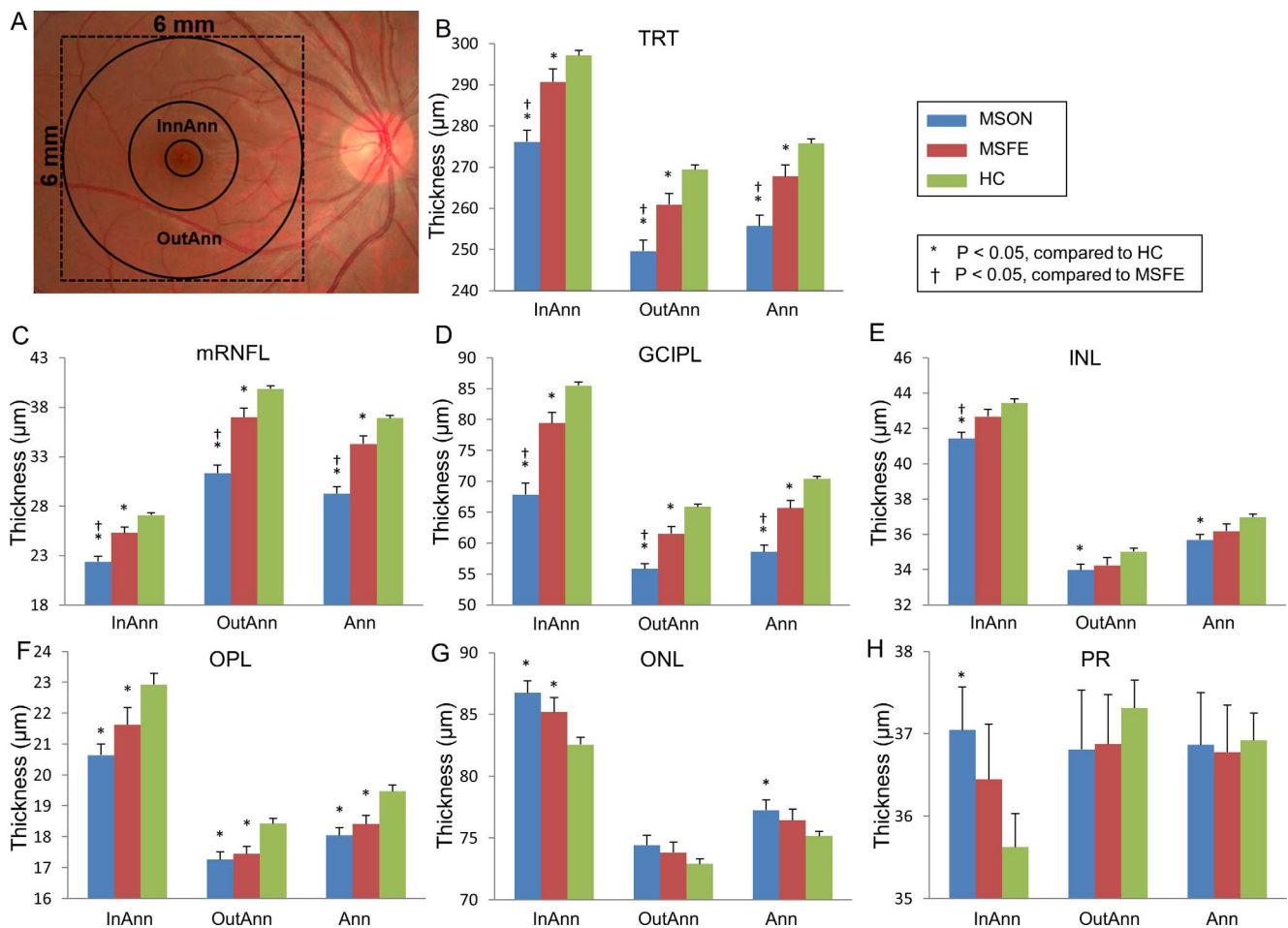
FIGURE 5. Annular thicknesses of the intraretinal layers in patients with MS compared with HC. (**A**) The central 1-mm zone of the fovea was removed. Three concentric rings with diameters of 1, 3, and 6 mm were used to divide the map into three zones. Significant thickness reductions were found in the TRT, mRNFL, and GCIPL in MSON compared with those of MSFE and HC in annular partitions using GEE models ($P < 0.05$). (**B–H**) GCIPL thickness in each annulus of TRT and six intraretinal layers. InnAnn, inner annulus; OutAnn, outer annulus; Ann, total annulus. *Bars* = SEs.

then MSON in the TRT, mRNFL, and GCIPL (Fig. 2). The subtraction maps showed that the thickness reductions occurred in MSON and MSFE eyes in all intraretinal layers, except for the ONL (Fig. 3).

Thickness Reduction Patterns of the GCIPL

To visualize the patterns of thickness reduction, the areas of the GCIPL with thickness alterations were determined in the thickness subtraction maps using different cutoff threshold settings. A horseshoe-like thickness reduction pattern was found in MSON (Fig. 4). In contrast, MSFE showed an island pattern located on the nasal side. Similar horseshoe-like thickness reduction patterns were also evident in the proportional thickness maps, which were calculated as (MSON-HC)/HC and (MSFE-HC)/HC (Fig. 4). The horseshoe-like thickness reduction was defined as the "U Zone" with a portion of an elliptic annulus (dimensions: 1.45 and 3.5 mm for the inner and outer vertical diameters, respectively, and 1.8 and 4.9 mm for the inner and outer horizontal diameters, respectively) around the fovea. The GCIPL thickness of the U Zone exhibited a significant reduction in MSON compared with that of MSFE and HC.

Topographic Thickness Partition and Analysis

Analyses of the annuli (Fig. 5), quadrants (Fig. 6), and sectors (Fig. 7) using the ETDRS partition revealed significant thickness reductions in the TRT, mRNFL, and GCIPL in MSON compared with those of MSFE and HC in partitions using GEE models ($P < 0.05$). The mRNFL and GCIPL thicknesses of all partitions were thinner in MSFE than those of HC ($P < 0.05$). The thicknesses of TRT in all annuli, quadrants, sectors, except for sectors inner inferior (II), inner temporal (IT), and OI were thinner in MSFE eyes than HC eyes ($P < 0.05$). Thickness alterations of the INL, OPL, outer nuclear layer (ONL), and PR were also found (Figs. 5–7).

Discrimination Power

The area under the receiver operating characteristic curve (AUC) was analyzed via counting a single eye and both eyes of each subject. The discrimination power of the GCIPL thickness in the U Zone was compared with the ETDRS partitions and the M Zone, which was previously defined in MS eyes without a history of ON.[15] The previously defined[15] M zone was located at nasal 1.98 mm and inferior 0.42 mm from the fovea with a circular area (Fig. 8). When a single eye for each group was counted, the GCIPL thickness of the U Zone had the best
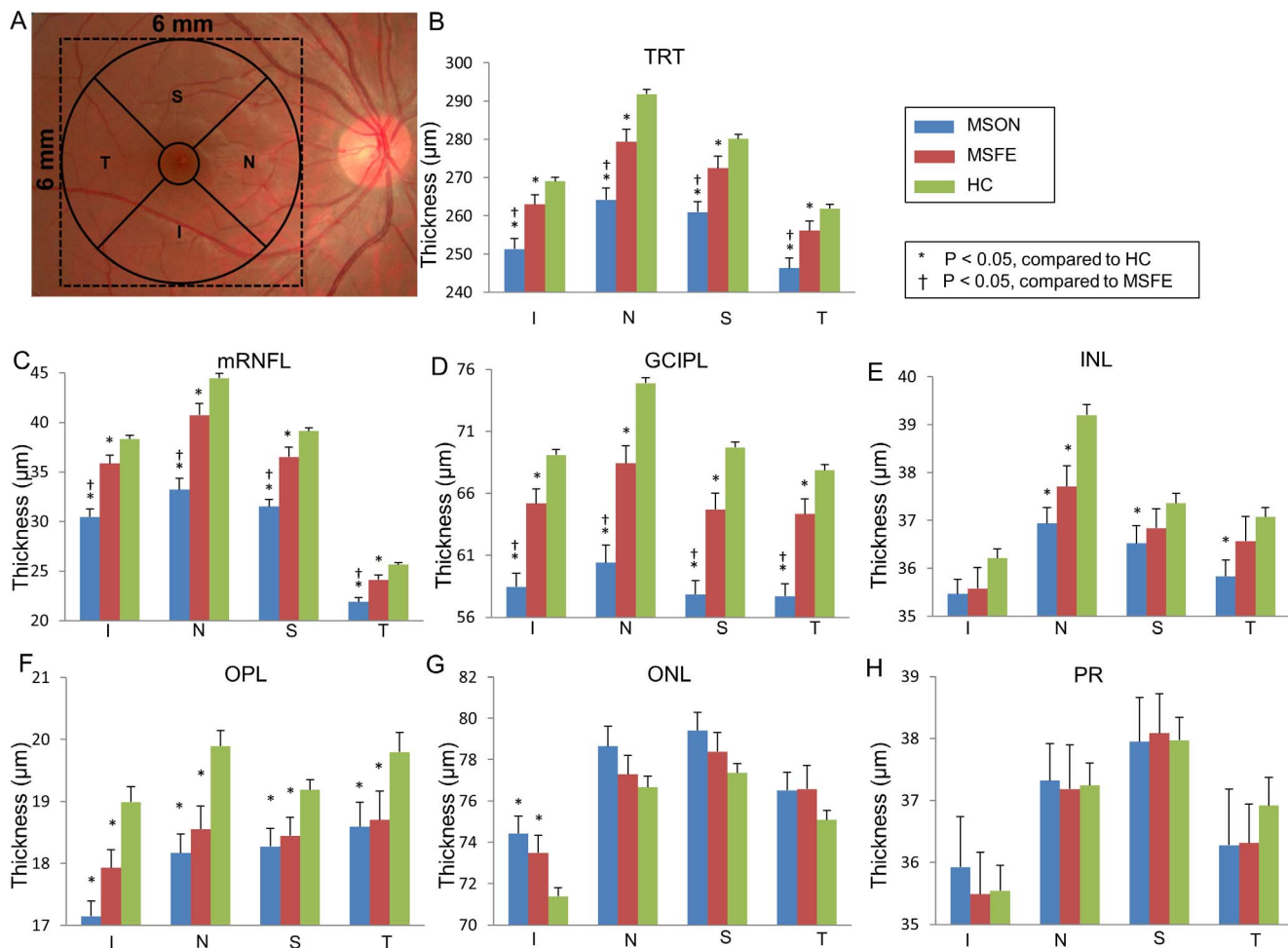
FIGURE 6. Quadrantal thicknesses of the intraretinal layers in patients with MS compared with controls. **(A)** After removal of the central 1-mm zone of the fovea, quadrantal division was performed using 45° and 135° medians according to the ETDRS definition. Significant thickness reductions were found in the TRT, mRNFL, and GCIPL in MSON compared with those of MSFE and HC in quadrantal partitions using GEE models ($P < 0.05$). **(B–H)** GCIPL thickness in each quadrant of TRT and six intraretinal layers. S, superior quadrant; T, temporal quadrant; N, nasal quadrant; I, inferior quadrant. *Bars* = SEs.

discrimination power (AUC = 0.97, sensitivity = 0.97, specificity = 0.83, with cutoff = 82.3 μm) in discriminating MSON eyes from HC eyes (Fig. 8). In contrast, the M Zone had the best discrimination power (AUC = 0.81, sensitivity = 0.81, specificity = 0.69, with cutoff = 84.0 μm) in discriminating MSFE from HC eyes (Fig. 8).

Analyses of the intereye differences in patients with a history of unilateral ON revealed that the thickness of the GCIPL in the nasal quadrant (GCIPL_N) had the best discrimination power (AUC = 0.86, sensitivity = 0.65, specificity = 0.92, with cutoff = 5.4 μm) in discriminating patients with MS and history of unilateral ON from HC, and the U Zone was ranked second, with a discrimination power of 0.85 (sensitivity = 0.69, specificity = 0.97, with cutoff = 6.2 μm). However, the M Zone was ranked 13th with a discrimination power of 0.79 (sensitivity = 0.77, specificity = 0.81, with cutoff = 7.1 μm) (Fig. 8).

Scatter plots of GCIPL thicknesses in the U Zone showed that the optimal cutoff discriminated all MSON eyes, except one eye (Fig. 9). However, MSFE were distributed on both sides of the cutoff. In contrast, the scatter plot of the intereye differences of the GCIPL in the U Zone in MS patients with a history of unilateral ON showed a moderate discrimination power to identify MS patients and exclude HC. Application of the optimal cutoff of GCIPL thickness in the U Zone

discriminated 16 eyes of the 26 MSFE eyes (62%) as MSON eyes.

Correlations Between OCT Measurements and Clinical Manifestations

The thickness of the U Zone was positively related to 2.5% LCLA ($r = 0.38$, $P < 0.05$) and 1.25% LCLA ($r = 0.57$, $P < 0.05$) in MS patients, which was slightly weaker compared with the GCIPL thickness in the inner superior sector (IS) (Fig. 10). The GCIPL thickness of the M Zone was significantly correlated to the Expanded Disability Status Scale (EDSS) ($r = -0.39$, $P < 0.05$). However, there were no significant relationships between disease duration and the OCT thickness measurements (r ranged from -0.20 to -0.14, $P > 0.05$).

DISCUSSION

This study was aimed to visualize topographic retinal thickness maps in patients with MS and a history of ON, and to evaluate their discrimination performance and relationships with clinical manifestations. The results of this study showed that thickness alterations of the GCIPL in the U Zone appeared to be specific to MSON eyes, which described the most profound
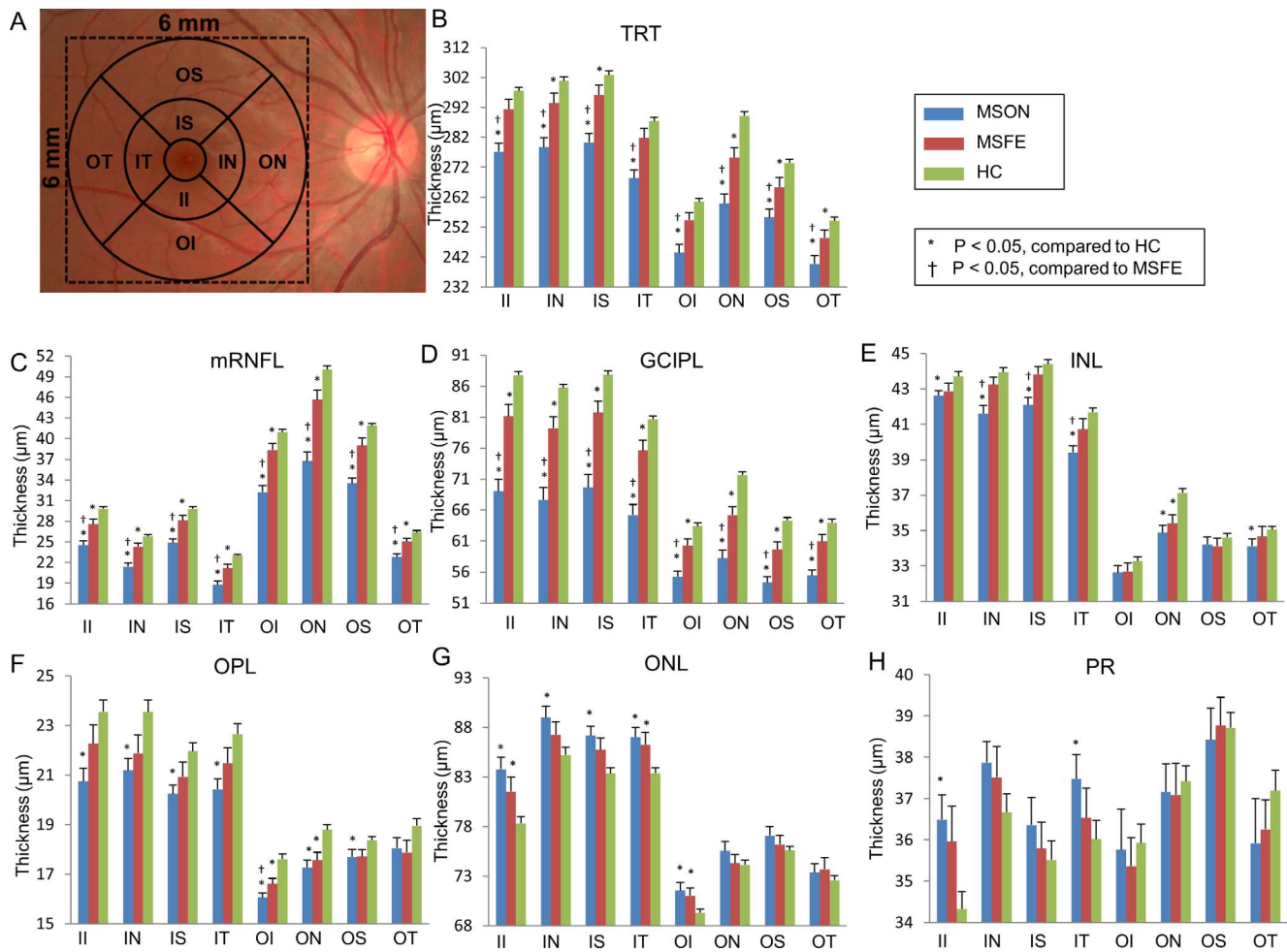
FIGURE 7. Sectoral thickness differences of the intraretinal layers in patients with MS compared with controls. (**A**) According to the ETDRS definition, the quadrantal division was performed using 45° and 135° medians. Three concentric rings with diameters of 1, 3, and 6 mm were used to divide the map into nine zones. The central 1-mm zone of the fovea was removed. Significant thickness reductions were found in the TRT, mRNFL, and GCIPL in MSON compared with those of MSFE and HC in sectoral partitions using GEE models ($P < 0.05$). (**B–H**) GCIPL thickness in each sector of TRT and six retina layers. II, inner inferior; IN, inner nasal; IT, inner temporal; OI, outer inferior; ON, outer nasal; OT, outer temporal; OS, outer superior. *Bars* = SEs.
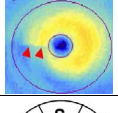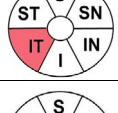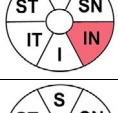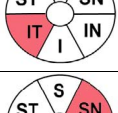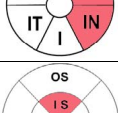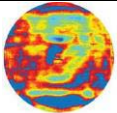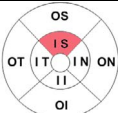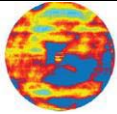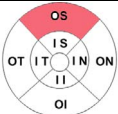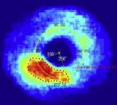
thickness alternation, and had the highest discrimination power and was positively correlated with LCLA. Therefore, the characteristic pattern of the GCIPL may be developed as an image marker for determining the history of ON as the evidence of damage to the optic nerve in MS. With the cutoff of 82.3-μm (equivalent to 4.5-μm thickness reduction), up to 97% of MSON eyes were discriminated from HC, which is a robust threshold for identifying optic lesions. This threshold may also be beneficial in identifying possible asymptomatic subclinical optic nerve lesions. The inclusion of optic nerve lesions as a site for imaging criteria for the diagnosis of MS is considered a high priority area for research by the magnetic resonance imaging in the MS study group.[23] Further validation using a large-scale study may be proved useful as a new add-on criterion for the diagnosis of MS.

The thickness alternations of the U Zone were found in MSON eyes based on the pattern and magnitude of the alteration. A profound change of up to 21 μm on average was typical, which is higher than the average change in the inner annulus defined by the commonly used elliptical z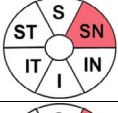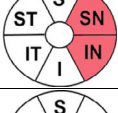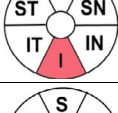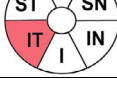one (−16.4 μm) according to a meta-analysis of multiple studies.[24] Therefore, the change in GCIPL thickness of an individual eye may be sufficient to establish the presence of optic nerve

lesions in MS, as shown in the present and previous studies.[22,24,25] In addition to the magnitude of the thickness reduction, the location of the changes may also be specific. The focal thickness reduction zone in the intraretinal layers generally represents the area that is most seriously affected by certain diseases (Table 2).[15,16,26-33] Different thickness reduction patterns were documented in different systemic conditions, such as Alzheimer's disease,[16] and ocular disorders, such as glaucoma.[26-28] These characteristic patterns often provide disease-specific information and better discrimination powers compared with averaged thickness.[27-29] Inferotemporal thinning of the GCIPL is reported in patients with glaucoma,[30] and inferonasal thinning of GCIPL is reported in patients with ethambutol-induced optic neuropathy.[26] Inferonasal and superonasal thinning of the GCIPL were reported in optic chiasmal compression caused by a pituitary adenoma.[28] A superior thinning of the GCIPL was also reported in patients with Alzheimer's disease.[16] Although the thickness alteration in the U Zone may be used to diagnose ON, whether the U Zone is specific to MSON remains untested since no other diseases were compared in the present study.

A previously published study demonstrated that focal thickness reduction in patients with MS and no history of

TABLE 2. Studies of GCIPL Thinning Pattern and AUC

| Authors	Disease	No. of Eyes	OCT Device	Analysis Tool	Thinning Pattern	AUC	Map
Hu et al. (present study)	Multiple sclerosis with optic neuritis vs. fellow eye vs. control	30 vs. 22 vs. 63	Custom-built UHR-OCT	Orion software	U zone	0.97	U Zone
Shi et al.[15] (2019)	Multiple sclerosis without optic neuritis vs. control	47 patients vs. 67 patients	Custom-built UHR-OCT	Orion software	M zone	0.77	M Zone
Lee et al.[27] (2018)	Glaucoma vs. optic neuropathy	67 vs. 73	Cirrus HD-OCT	Built-in software	Temporal raphe sign	0.811	
Chen et al.[30] (2019)	Preperimetric glaucoma vs. control	67 vs. 67	SD-OCT	Built-in software	Inferotemporal	0.784	
Lee et al.[26] (2018)	Ethambutol-induced optic neuropathy vs. control	28 vs. 100	Cirrus SD-OCT	Built-in software	Inferonasal	0.833	
Sharifipour et al.[29] (2017)	Glaucoma vs. control	101 vs. 69	Cirrus HD-OCT	Built-in software	Inferotemporal	0.944	
Yum et al.[28] (2016)	Optic chiasmal compression by a pituitary adenoma vs. control	46 vs. 32	Cirrus HD-OCT	Built-in software	Inferonasal, superonasal	0.965, 0.958	
Shao et al.[16] (2018)	Alzheimer's disease vs. control	25 vs. 21	Custom-built UHR-OCT	Orion software	Inner superior		
Shao et al.[16] (2018)	Mild cognitive impairment vs. control	24 vs. 21	Custom-built UHR-OCT	Orion software	Outer superior		
Shin et al.[31] (2018)	Primary open-angle glaucoma	292	Cirrus HD-OCT	MATLAB software	Inferotemporal region (250°–339°) at 2.08 mm from the fovea		
Balducci et al.[32] (2016)	Acute Leber's hereditary optic neuropathy vs. control (1 month)	6 vs. 11	Cirrus HD-OCT	Built-in software	Superonasal	0.9545	
Balducci et al.[32] (2016)	Acute Leber's hereditary optic neuropathy vs. control (2 month)	6 vs. 11	Cirrus HD-OCT	Built-in software	Inferonasal, superonasal	1.0, 1.0	
Cheung et al.[33] (2015)	Alzheimer's disease vs. control	100 vs. 123	Cirrus HD-OCT	Built-in software	Inferior	0.722	
Cheung et al.[33] (2015)	Mild cognitive impairment vs. control	41 vs. 123	Cirrus HD-OCT	Built-in software	Inferotemporal	0.688	
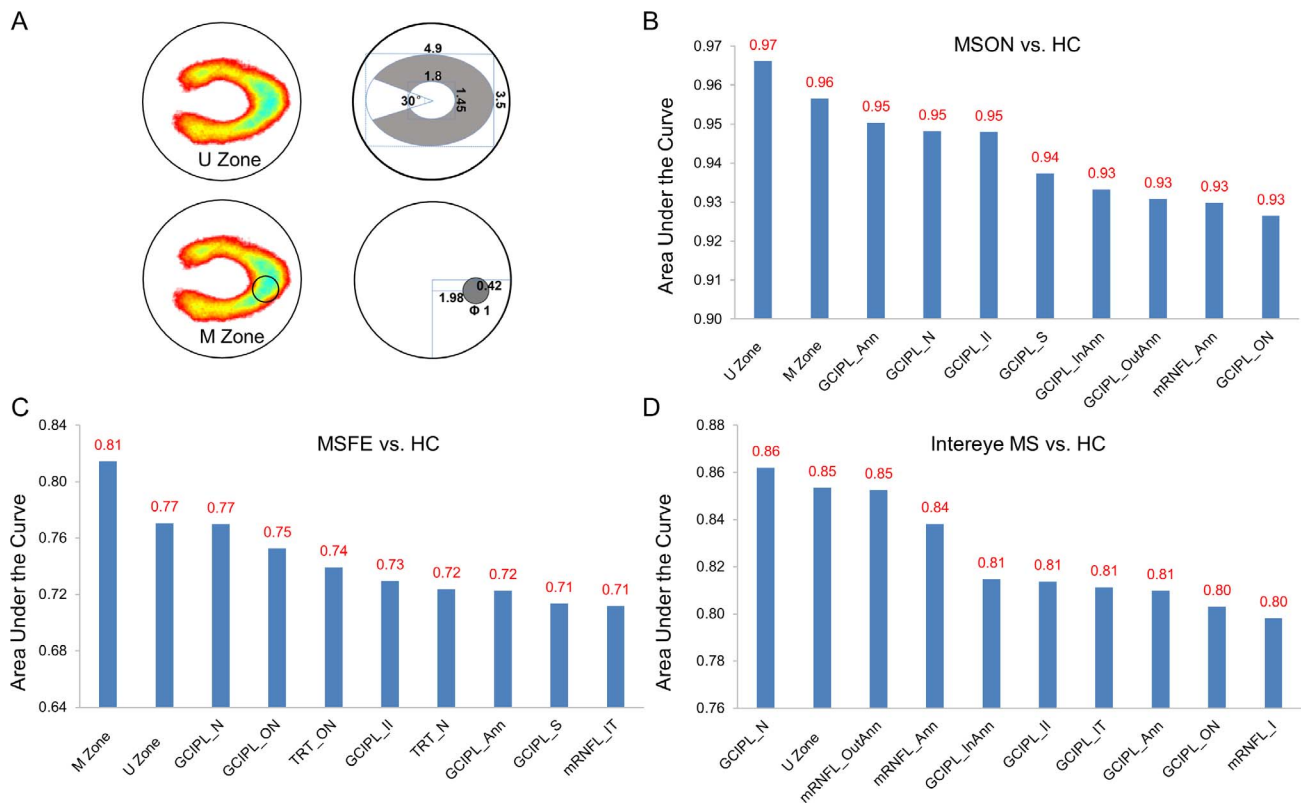
FIGURE 8. Discrimination power of the GCIPL thickness. (**A**) Schematic diagram and location of the U Zone and M Zone of GCIPL thickness. Data are presented in millimeters. (**B**) Calculated from MSON and HC eyes (MSON: $N = 34$ eyes, HC: $N = 126$ eyes), the U Zone had the best discrimination power (AUC = 0.97) in discriminating MSON eyes from HC eyes. (**C**) Calculated from MSFE and HC eyes (MSFE: $N = 26$ eyes; HC: $N = 126$ eyes), the M Zone had the best discrimination power (AUC = 0.81) in discriminating MSFE eyes from HC eyes. (**D**) Calculated from the intereye differences of GCIPL in MS patients with a history of unilateral ON (MS: $N = 26$ patients, HC: $N = 63$ subjects), the thickness of the GCIPL in the nasal quadrant (GCIPL_N) had the best discrimination power (AUC = 0.86, sensitivity = 0.65, specificity = 0.92, with cutoff = 5.4 μm) in discriminating patients with MS and a history of unilateral ON from HC, and the U Zone ranked second with a discrimination power of 0.85.

ON was limited to a small zone in the nasal-inferior region, named the M Zone.[15] A similar M Zone existed in MSFE eyes, and the thickness reduction zone expanded to a horseshoe-shaped region in MSON eyes. The similarities in the thickness reductions (e.g., horseshoe shape with the small thickness deductions shown in Fig. 4B) with a much smaller scale in MSFE eyes also support the speculation, but much more profound alterations were observed in the MSON eyes. This result indicates that the specific topographic thickness patterns may be used to identify neural damage due to ON in patients with MS and may be used to determine possible subclinical ON.

The present study observed topographic changes between MSFE and MSON eyes, such as focal thickness reductions of the GCIPL in the M Zone and U Zone, respectively. Acute ON causes a profound but heterogeneous thinning of intraretinal layers in patients with MS,[24] which indicates extensive damage of the ganglion cells due to local optic nerve inflammation.

TABLE 3. Studies of Intereye Difference for MSON

Authors	MSON (Patient)	Control (Subject)	OCT Device	Retina Layer	Intereye Difference Cutoff	Sensitivity, %	Specificity, %
Hu et al. (present study)	30	63	UHR-OCT	U Zone	6 μm (optimized)	69	97
					4 μm	73	86
					3 μm	77	81
Nolan et al.[14]	45	31	SD-OCT	pRNFL Ave	5 μm	76	75
					6 μm	62	81
Coric et al.[11]	62	63	SD-OCT	GCIPL percentage	20%	34	100
					6%	70	97
Xu et al.[12]	51*	233	HD-OCT	pRNFL Ave	9 μm	73	
				GCIPL Ave	6 μm	96	
Nolan et al.[13]	477	368	SD-OCT	pRNFL Ave	5 μm	71	65
				GCIPL Ave	4 μm	68	77

* Including patients with various disorders such as MS (51%), idiopathic (41%), and neuromyelitis optica spectrum disorder (8%).
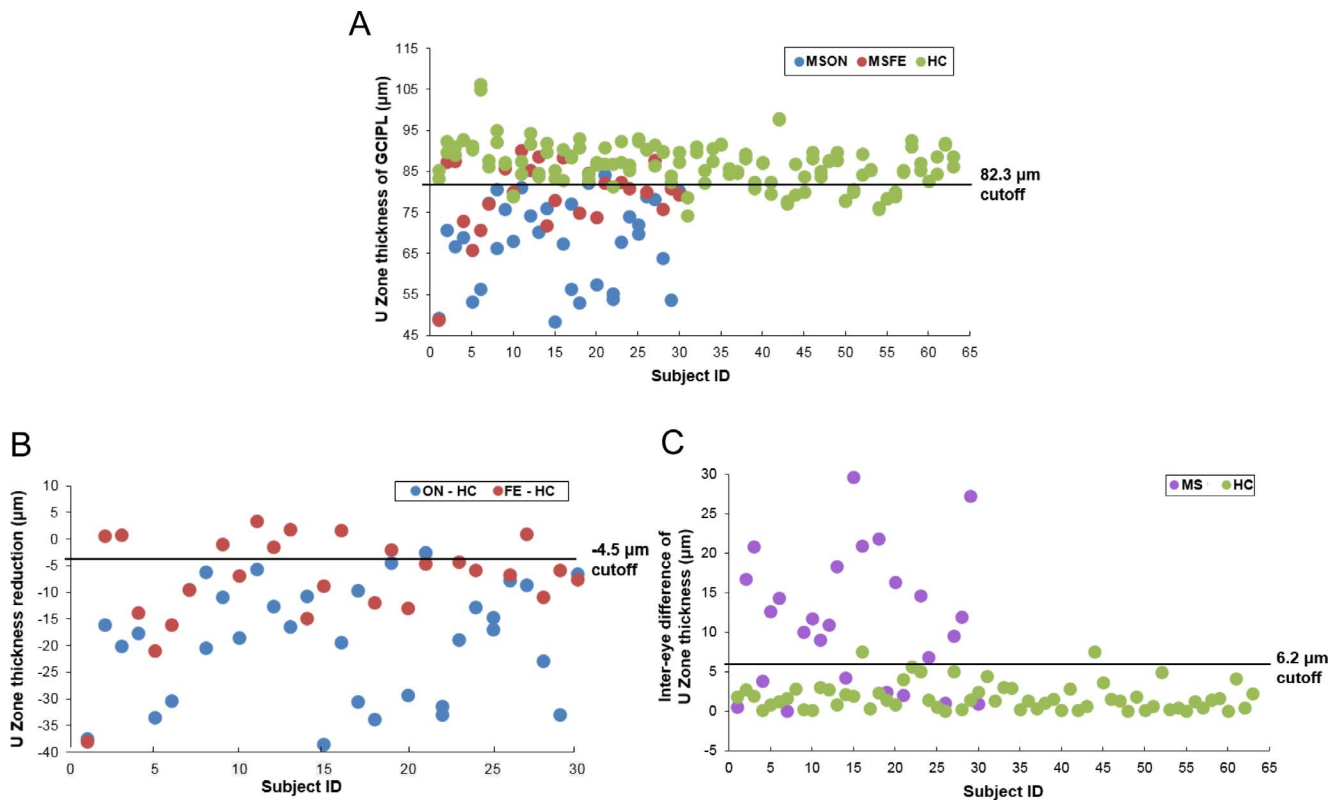
FIGURE 9. Scatter plots with the cutoff of GCIPL thickness in the U Zone. (**A**) U Zone thickness of each eye. The *horizontal line* is drawn at the 82.3-μm cutoff point, which is the optimal cutoff for the best discrimination power of MSON from HC eyes. (**B**) U Zone thickness reduction of each eye in the MSON and MSFE groups compared with HC. The *horizontal line* is drawn at the −4.5-μm cutoff point, which is the difference of the U Zone thickness cutoff and the average thickness of HC eyes. (**C**) Intereye differences in U Zone thickness in MS and HC subjects. The *horizontal line* is drawn at the 6.2-μm cutoff point, which is the optimal cutoff for discriminating MS patients with a history of unilateral ON.

This damage may explain why the focal thinning zone expanded from a circular area (i.e., the M Zone) to a horseshoe-shaped area (i.e., the U Zone). The reduction in the U Zone occurred almost completely in the annulus, where the thickest GCIPL band between the inner and outer annuli exists. The reduction was not proportional to the baseline thickness of the HC eyes, which may indicate that the U Zone is a vulnerable region to ON damage. Whereas the M Zone had the best performance in differentiating eyes with MSFE from HC, and it was similar to MSNON eyes,[15] which may indicate that MSFE and MSNON share similar characteristics of focal thickness reduction and may be at similar disease stages. The focal thinning of the GCIPL in the M Zone in MSFE eyes echoes previous findings that mitochondrial dysfunction contributes to MS pathophysiology.[34–36] Furthermore, the location of the M Zone is similar to the focal thinning of the GCIPL from mitochondrial optic neuropathies,[37,38] and smaller axons were more profoundly damaged in patients with MS.[39,40] The M Zone thickness negatively correlated to EDSS in patients with MSON, with an *r* value of 0.39, which was less than MSNON (*r* = 0.59) found in our previous study.[15] This phenomenon echoes the findings that the pRNFL and GCIP thicknesses derived from eyes with a history of ON may correlate less with brain or brain-substructure volumes than eyes without a previous history of ON.[9,41–43]

In clinical practice, due to excellent visual function recovery, including visual acuity and visual fields, the prior ON is sometimes not confirmed. Also, subclinical optic neuropathy due to the diffuse demyelination that is present in MS[5] may result in a similar degree of average thinning of the pRNFL and GCIPL compared with MSON eyes. The intereye

variability of pRNFL and GCIPL thicknesses were reported to have better discrimination power to identify possible prior ON (Table 3).[3,11,12,14] However, the threshold criteria of the intereye differences only exhibited moderate discrimination powers, except for the study of Xu et al.[12] Using 6 μm derived from 99th percentile of a normal population (233 subjects), Xu et al.[12] reported 96% sensitivity to determine prior ON in mixed patients including MS (51%), idiopathic (41%), and neuromyelitis optica spectrum disorder (8%). Because of the mixed etiology of ON, the cutoff and its associated sensitivity may not be recommended as a routine tool for diagnosing ON in patients with MS.[3] However, a recent international study reported an optimal intereye difference threshold of the GCIPL for identifying prior unilateral ON,[13] and the sensitivity of a 4-μm cutoff of GCIPL yielded similar results in previous studies.[11,14] Coric et al.[11] studied intereye GCIPL percentage difference normalized to the absolute thickness level of retinal layers and found that a 6% intereye difference in the GCIPL had 62% sensitivity. Nolan et al.[13] reported a 4-μm intereye GCIPL difference to identify prior ON based on a large sample size (477 patients with unilateral ON and 253 HC subjects). The intereye difference (4 μm) of the U Zone thickness provided a 73% sensitivity in the present study, and the cutoff of 3 μm of the U Zone thickness provided 77% sensitivity, which are slightly better than previous studies,[11,13,14] except for the study of Xu et al.[12] Notably, the moderate sensitivity of the GCIPL in determining prior ON may be due to the ubiquitous occurrence of subclinical ON, which is often asymptomatic.[3] Approximately one-third of patients with MS with intereye differences greater than 4 μm reported no history of ON. These patients may have subclinical ON. If subclinical ON occurred in
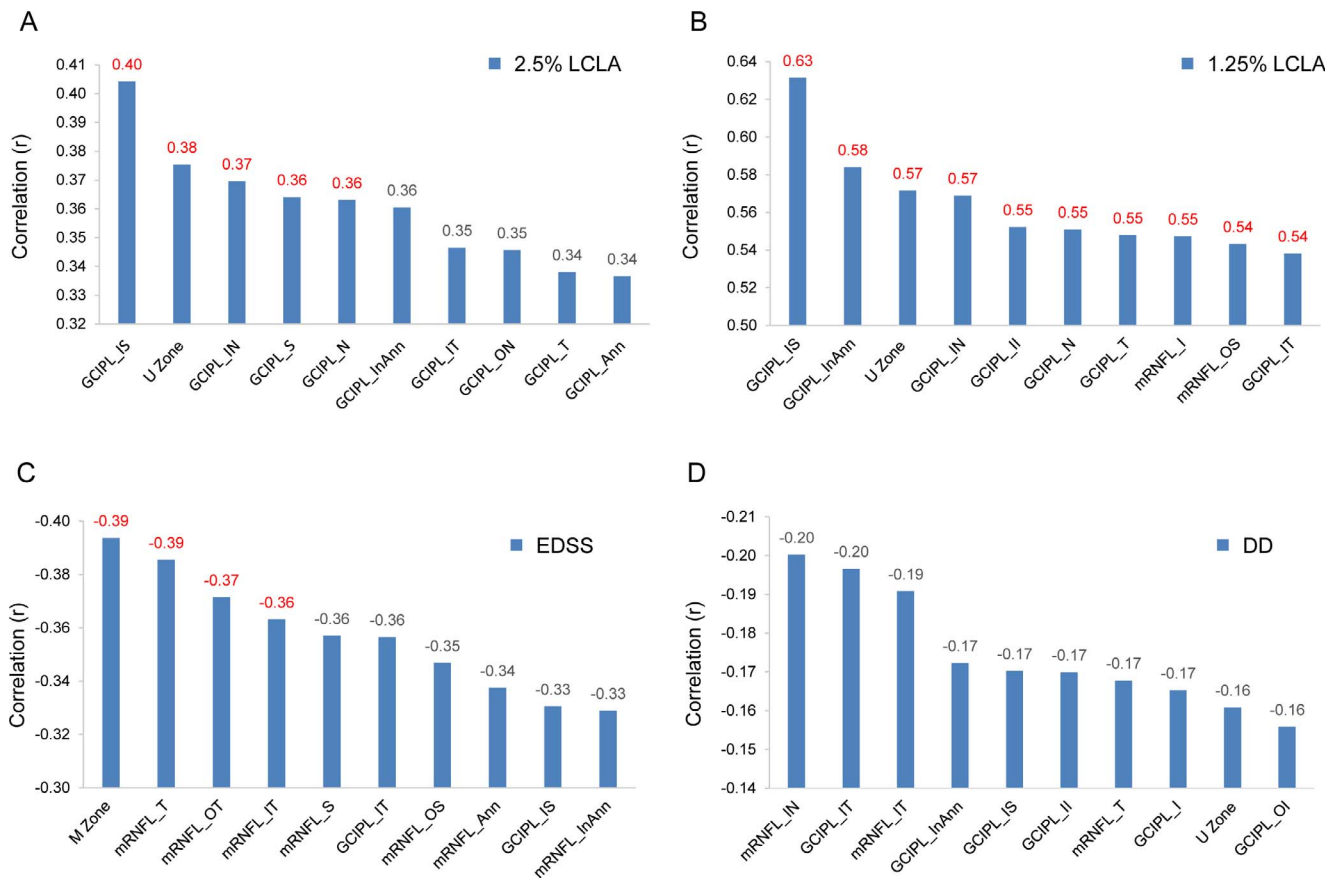
FIGURE 10. Relationships between OCT thickness measurements and clinical manifestations. (**A**) The thickness of the U Zone was positively related to 2.5% LCLA ($r = 0.38$, $P < 0.05$), which was less than the GCIPL_IS. (**B**) The thickness of the U Zone was also positively related to the 1.25% LCLA ($r = 0.57$, $P < 0.05$), which was slightly weaker than some of the other partitions. (**C**) The thickness of the M Zone was negatively related to EDSS ($r = -0.39$, $P < 0.05$). (**D**) There were no significant relationships between DD and OCT thickness measurements. DD, disease duration.

the fellow eyes, the intereye differences may be diminished, which may explain our finding that approximately 6-fold of fellow eyes had GCIPL thickness in the U Zone below the cutoff value (i.e., 82.3 µm or reduction 4.5 µm compared with HC). Therefore, combining the cutoff of the GCIPL of individual eyes and the cutoff of intereye thickness difference is recommended for identifying optic nerve lesions, including subclinical optic nerve pathology.

There are several limitations to the present study. First, although MSON in our study had a history of ON, we do not know whether the fellow eye had subclinical ON. Second, our study used a custom-built UHR-OCT, which is not used in routine clinics. Although the axial resolution (i.e., ~3 µm) of our UHR-OCT is higher than most commercial OCT devices (commonly ~5 µm), the scan speed is 24 Khz, which is slower than currently commercial OCT devices (i.e., 70–100 Khz). Further update of the scan speed in our system is needed. Furthermore, the results obtained from the custom built UHR-OCT may limit the generalization of our current findings. However, the Orion Software used in the present study has been adapted in commercial OCT devices such as Zeiss Cirrus HD-OCT (with special data exportation),[44,45] Topcon 3D-1000 (Topcon Medical Systems, Inc., Oakland, NJ, USA),[46] and Spectralis SD OCT (Heidelberg Engineering, Heidelberg, Germany).[47] Our study can be repeated using these commercial OCT devices and the Orion software.[44–47] In addition, the visualized thickness reduction patterns may provide a reference for the clinical interpretation of OCT images using

clinically available OCT devices. Third, the segmentation of intraretinal layers of each B-scan of the volumetric data set was not verified by the investigators, which constitutes a limitation. Visual inspection and possible manual correction of each B-scan may help reduce the segmentation errors. Fourth, the sample size was small, compared with recent studies involving hundreds of patients,[11–13] which may cast a risk of bias. However, the visualization of the focal alteration of topographic thicknesses in patients with ON may provide useful information for designing future independent population based studies to refine the topographic alteration of the intraretinal layers in patients with ON. Fifth, we did not perform follow-up of these patients. Longitudinal studies may further reveal the time course of focal thinning.

In conclusion, the horseshoe-like thickness reduction of the GCIPL appeared to be an ON-specific focal thickness alteration with the highest discrimination power of MSON. The characteristic changes may represent the vulnerable regions affected by ON in patients with MS and may be developed into an image marker for the diagnosis of prior ON.

References

1. Browne P, Chandraratna D, Angood C, et al. Atlas of multiple sclerosis 2013: a growing global problem with widespread inequity. *Neurology*. 2014;83:1022–1024.

2. Noyes K, Weinstock-Guttman B. Impact of diagnosis and early treatment on the course of multiple sclerosis. *Am J Manag Care*. 2013;19:s321–s331.

3. Saidha S, Naismith RT. Optical coherence tomography for diagnosing optic neuritis: are we there yet? *Neurology*. 2019; 92:253–254.

4. Balcer LJ. Clinical practice. Optic neuritis. *N Engl J Med*. 2006;354:1273–1280.

5. Ikuta F, Zimmerman HM. Distribution of plaques in seventy autopsy cases of multiple sclerosis in the United States. *Neurology*. 1976;26:26–28.

6. Button J, Al-Louzi O, Lang A, et al. Disease-modifying therapies modulate retinal atrophy in multiple sclerosis: a retrospective study. *Neurology*. 2017;88:525–532.

7. Martinez-Lapiscina EH, Arnow S, Wilson JA, et al. Retinal thickness measured with optical coherence tomography and risk of disability worsening in multiple sclerosis: a cohort study. *Lancet Neurol*. 2016;15:574–584.

8. Saidha S, Syc SB, Durbin MK, et al. Visual dysfunction in multiple sclerosis correlates better with optical coherence tomography derived estimates of macular ganglion cell layer thickness than peripapillary retinal nerve fiber layer thickness. *Mult Scler*. 2011;17:1449–1463.

9. Saidha S, Al-Louzi O, Ratchford JN, et al. Optical coherence tomography reflects brain atrophy in multiple sclerosis: a four-year study. *Ann Neurol*. 2015;78:801–813.

10. Brandt AU, Martinez-Lapiscina EH, Nolan R, Saidha S. Monitoring the course of MS with optical coherence tomography. *Curr Treat Options Neurol*. 2017;19:15.

11. Coric D, Balk LJ, Uitdehaag BMJ, Petzold A. Diagnostic accuracy of optical coherence tomography inter-eye percentage difference for optic neuritis in multiple sclerosis. *Eur J Neurol*. 2017;24:1479–1484.

12. Xu SC, Kardon RH, Leavitt JA, et al. Optical coherence tomography is highly sensitive in detecting prior optic neuritis. *Neurology*. 2019;92:e527–e535.

13. Nolan RC, Liu M, Akhand O, et al. Optimal inter-eye difference thresholds by OCT in MS: an international study. *Ann Neurol*. 2019;85:618–629.

14. Nolan RC, Galetta SL, Frohman TC, et al. Optimal intereye difference thresholds in retinal nerve fiber layer thickness for predicting a unilateral optic nerve lesion in multiple sclerosis. *J Neuroophthalmol*. 2018;38:451–458.

15. Shi C, Jiang H, Gameiro GR, et al. Visual function and disability are associated with focal thickness reduction of the ganglion cell-inner plexiform layer in patients with multiple sclerosis. *Invest Ophthalmol Vis Sci*. 2019;60:1213–1223.

16. Shao Y, Jiang H, Wei Y, et al. Visualization of focal thinning of the ganglion cell-inner plexiform layer in patients with mild cognitive impairment and Alzheimer's disease. *J Alzheimers Dis*. 2018;64:1261–1273.

17. Tan J, Yang Y, Jiang H, et al. The measurement repeatability using different partition methods of intraretinal tomographic thickness maps in healthy human subjects. *Clin Ophthalmol*. 2016;10:2403–2415.

18. Polman CH, Reingold SC, Banwell B, et al. Diagnostic criteria for multiple sclerosis: 2010 revisions to the McDonald criteria. *Ann Neurol*. 2011;69:292–302.

19. Balcer LJ, Baier ML, Cohen JA, et al. Contrast letter acuity as a visual component for the Multiple Sclerosis Functional Composite. *Neurology*. 2003;61:1367–1373.

20. Wei Y, Jiang H, Shi Y, et al. Age-related alterations in the retinal microvasculature, microcirculation, and microstructure. *Invest Ophthalmol Vis Sci*. 2017;58:3804–3817.

21. Lin Y, Jiang H, Liu Y, et al. Age-related alterations in retinal tissue perfusion and volumetric vessel density. *Invest Ophthalmol Vis Sci*. 2019;60:685–693.

22. Britze J, Pihl-Jensen G, Frederiksen JL. Retinal ganglion cell analysis in multiple sclerosis and optic neuritis: a systematic review and meta-analysis. *J Neurol*. 2017;264:1837–1853.

23. Filippi M, Rocca MA, Ciccarelli O, et al. MRI criteria for the diagnosis of multiple sclerosis: MAGNIMS consensus guidelines. *Lancet Neurol*. 2016;15:292–303.

24. Petzold A, Balcer LJ, Calabresi PA, et al. Retinal layer segmentation in multiple sclerosis: a systematic review and meta-analysis. *Lancet Neurol*. 2017;16:797–812.

25. Petzold A, de Boer JF, Schippling S, et al. Optical coherence tomography in multiple sclerosis: a systematic review and meta-analysis. *Lancet Neurol*. 2010;9:921–932.

26. Lee JY, Choi JH, Park KA, Oh SY. Ganglion cell layer and inner plexiform layer as predictors of vision recovery in ethambutol-induced optic neuropathy: a longitudinal OCT analysis. *Invest Ophthalmol Vis Sci*. 2018;59:2104–2109.

27. Lee J, Kim YK, Ha A, et al. Temporal raphe sign for discrimination of glaucoma from optic neuropathy in eyes with macular ganglion cell-inner plexiform layer thinning. *Ophthalmology*. 2019;126:1131–1139.

28. Yum HR, Park SH, Park HY, Shin SY. Macular ganglion cell analysis determined by cirrus HD optical coherence tomography for early detecting chiasmal compression. *PLoS One*. 2016;11:e0153064.

29. Sharifipour F, Morales E, Lee JW, et al. Vertical macular asymmetry measures derived from SD-OCT for detection of early glaucoma. *Invest Ophthalmol Vis Sci*. 2017;58:4310–4317.

30. Chen MJ, Yang HY, Chang YF, et al. Diagnostic ability of macular ganglion cell asymmetry in preperimetric glaucoma. *BMC Ophthalmol*. 2019;19:12.

31. Shin JW, Sung KR, Park SW. Patterns of progressive ganglion cell-inner plexiform layer thinning in glaucoma detected by OCT. *Ophthalmology*. 2018;125:1515–1525.

32. Balducci N, Savini G, Cascavilla ML, et al. Macular nerve fibre and ganglion cell layer changes in acute Leber's hereditary optic neuropathy. *Br J Ophthalmol*. 2016;100:1232–1237.

33. Cheung CY, Ong YT, Hilal S, et al. Retinal ganglion cell analysis using high-definition optical coherence tomography in patients with mild cognitive impairment and Alzheimer's disease. *J Alzheimers Dis*. 2015;45:45–56.

34. Dutta R, McDonough J, Yin X, et al. Mitochondrial dysfunction as a cause of axonal degeneration in multiple sclerosis patients. *Ann Neurol*. 2006;59:478–489.

35. Su KG, Banker G, Bourdette D, Forte M. Axonal degeneration in multiple sclerosis: the mitochondrial hypothesis. *Curr Neurol Neurosci Rep*. 2009;9:411–417.

36. Witte ME, Mahad DJ, Lassmann H, van HJ. Mitochondrial dysfunction contributes to neurodegeneration in multiple sclerosis. *Trends Mol Med*. 2014;20:179–187.

37. Yu-Wai-Man P, Votruba M, Burte F, et al. A neurodegenerative perspective on mitochondrial optic neuropathies. *Acta Neuropathol*. 2016;132:789–806.

38. Carelli V, la MC, Sadun AA. Mitochondrial dysfunction in optic neuropathies: animal models and therapeutic options. *Curr Opin Neurol*. 2013;26:52–58.

39. Evangelou N, Konz D, Esiri MM, et al. Size-selective neuronal changes in the anterior optic pathways suggest a differential susceptibility to injury in multiple sclerosis. *Brain*. 2001;124: 1813–1820.

40. Ganter P, Prince C, Esiri MM. Spinal cord axonal loss in multiple sclerosis: a post-mortem study. *Neuropathol Appl Neurobiol*. 1999;25:459–467.

41. Siger M, Dziegielewski K, Jasek L, et al. Optical coherence tomography in multiple sclerosis: thickness of the retinal nerve fiber layer as a potential measure of axonal loss and brain atrophy. *J Neurol*. 2008;255:1555–1560.

42. Zimmermann H, Freing A, Kaufhold F, et al. Optic neuritis interferes with optical coherence tomography and magnetic resonance imaging correlations. *Mult Scler*. 2013;19:443–450.

43. Saidha S, Sotirchos ES, Oh J, et al. Relationships between retinal axonal and neuronal measures and global central nervous system pathology in multiple sclerosis. *JAMA Neurol*. 2013;70:34–43.

44. Behbehani R, Abu Al-Hassan A, Al-Salahat A, et al. Optical coherence tomography segmentation analysis in relapsing remitting versus progressive multiple sclerosis. *PLoS One*. 2017;12:e0172120.

45. Keller J, Oakley JD, Russakoff DB, et al. Changes in macular layers in the early course of non-arteritic ischaemic optic neuropathy. *Graefes Arch Clin Exp Ophthalmol*. 2016;254: 561–567.

46. Lamin A, Oakley JD, Dubis AM, Russakoff DB, Sivaprasad S. Changes in volume of various retinal layers over time in early and intermediate age-related macular degeneration. *Eye (Lond)*. 2019;33:428–434.

47. Hecht I, Yeshurun I, Bartov E, et al. Retinal layers thickness changes following epiretinal membrane surgery. *Eye (Lond)*. 2018;32:555–562.